

Characterization of CO₂ miscible/immiscible flooding in low-permeability sandstones using NMR technology and VOF method

Wenlian Xiao^{1*}, Jitian Ren¹, Wanfen Pu¹, Yanbing Tang¹, Qianrui Cheng¹

1 State Key Laboratory of Oil and Gas Reservoir Geology and Exploitation, Southwest Petroleum University

(*Wenlian Xiao: joshxiao@163.com)

ABSTRACT

CO₂ flooding is considered as one of the most effective enhanced oil recovery (EOR) methods in low-permeability reservoirs. In our work, we studied CO₂ miscible/immiscible flooding in low-permeability sandstones, using nuclear magnetic resonance (NMR) and volume of fluid (VOF) method. The experimental results indicated that the oil recovery after CO₂ miscible flooding is 68.13%, which is twice as much as the one after CO₂ immiscible flooding; oil in large pores is mainly displaced in the process of CO₂ immiscible flooding, whereas in the case of CO₂ miscible flooding, the oil comes from all kinds of pores. On the basis of VOF simulation results, it was found that oil recovery after CO₂ miscible flooding is also two times the one after CO₂ immiscible flooding, which are dependent on the characteristic of CO₂-oil contact. Moreover, oil recovery of CO₂ miscible/immiscible flooding significantly decreased with the increase of oil viscosity. The interesting observation is that piston displacement happened at the injection part and finger displacement did at the production part during CO₂ miscible flooding. In the end, we found that CO₂ storage rate of miscible flooding is higher than that of immiscible flooding, and CO₂ storage rate also significantly decreased with the increase of oil viscosity.

Keywords: miscible/immiscible, NMR; VOF, oil recovery, CO₂ storage

NONMENCLATURE

Abbreviations

APEN Applied Energy

Symbols

n Year

1. INTRODUCTION

Low-permeability oil reservoirs are abundant in resources and widely distributed, with proven reserves accounting for 54% of geological reserves, which has become the main target of oil development^[1, 2]. There are some problems in water flooding period such as low oil recovery and pressure, rapid increase in water cut due to the small pores and strong heterogeneity^[3-5]. Compared with water flooding, CO₂ flooding is superior in maintaining reservoir pressure^[6], expanding swept volume and enhancing oil recovery, especially CO₂ miscible flooding^[7, 8]. CO₂ would dissolve in oil, causing oil to expand and displacing residual oil at the blind end of pores^[9-11]. At the same time, the dissolved CO₂ also would reduce the interfacial tension between oil and CO₂, and improve the flow of oil^[12]. Currently, research on the flow of CO₂ and oil in low-permeability reservoirs is still focused on laboratory work. For example, Wei et al. used NMR method to study the CO₂ miscible flooding. Piston displacement appeared in CO₂ miscible flooding. And oil in large pores was displaced in CO₂ miscible flooding^[13]. Cai et al. studied the distribution of oil in CO₂ miscible flooding and immiscible flooding, and found that the recovery rate of miscible displacement is twice that of immiscible flooding. It can be seen that the experimental results of CO₂ miscible flooding are rich, but the experimental results mostly show the coupling effect of multiple factors^[14]. Moreover, the tested samples are limited to the flow experiment process and cannot be reused.

Therefore, it is difficult to directly study the influence of various factors on CO₂ flooding through laboratory experiments alone. Core numerical simulation has unique advantages in comparison. At present, digital cores numerical simulation mainly includes pore network simulation methods^[15-17], LBM methods^[18], and Navier Stokes methods. Compared to the pore network simulation method, the Navier Stokes simulation method extracts the real pore throat based on digital rock cores,

establishes a pore throat mesh model, and directly solves the Navier Stokes equation.

At the same time, compared with the LBM method, the Navier Stokes method can directly calculate the fluid stress status, facilitate the analysis of the mechanical mechanism of fluid flow, and meet the needs of reservoir development mechanism analysis. The VOF method based on Navier Stokes equation was first proposed by Hirt and Nichols in the late 1970s, and is mainly used in aerodynamics and fluid mechanics. There are few reports on the simulation of pore size in oil and gas reservoirs. Martin J. Blunt et al. directly carried out the numerical simulation of microporosity under the condition of low Reynolds number on the digital core image based on this method, but he only considered single-phase fluid, which is only applicable to low-speed flow^[19]. Sun et al. analyzed the characteristics of oil water flow based on digital core VOF simulation and evaluated the effectiveness of water flooding. Injected water flowed along the dominant channel, and the growth of sweep coefficient gradually slowed down to a stable state^[20]. It was found that the VOF method based on the Navier Stokes equation for CO₂ flooding has not been reported yet.

In this study, CO₂ flooding experiments and VOF simulation were conducted to compare the EOR, flow and CO₂ storage in miscible and immiscible flooding. Subsequently, the method was used to simulated the effect of oil viscosity on CO₂ flow and oil recovery.

2. MATERIAL AND METHODS

2.1 Materials

The low permeability core samples in this work were about 10cm in length and 2.54cm in diameter, collected from a production in low permeability bottom water reservoir in China. The core samples were first cleaned with toluene, then dried in 333.15K for 48h. Permeability and porosity were tested by helium under confining pressure of 4.5MPa and pore pressure of 1.5MPa. The physical properties were listed in Table 1 The oil sample was formation oil. The minimum miscibility pressure of oil-CO₂ was 20.32MPa obtained by slim tube method.

Table 1 Physical properties of the core samples

Sample	Φ(%)	k (mD)	Injected rate (mL/min)	Back pressure (MPa)
1	12.40	0.50	0.05	5
2	10.22	0.37	0.05	25

2.2 Experimental procedures

The experimental flow chart of CO₂ flooding system was displayed in Fig. 1, which consisted of four systems: NMR system, a core holder, fluid injecting system and heating system. Fig. 1b showed fluid injection system. The fluid injection system included two intermediate containers, each containing CO₂ and oil. The intermediate container was connected to one ISCO pump with a six-way valve. The NMR system was displayed in Fig. 1c. The waiting time was 5000ms, the echo interval was 0.5ms, and the scanning number was 64 for nuclear magnetic resonance, respectively.

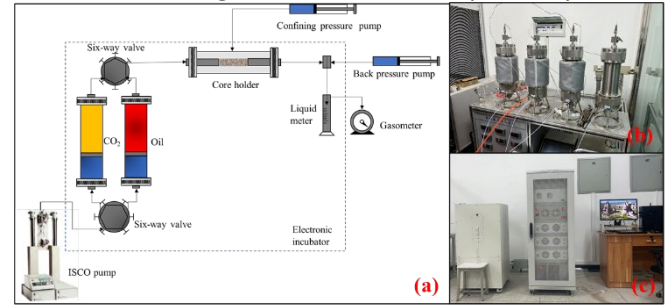


Fig. 1. schematic of NMR CO₂ flooding experimental device

The experimental steps for NMR CO₂ flooding were as follows: (1) Core samples were vacuumized for 2 hours and saturated with oil at 20MPa for 48 hours and tested initial T_2 spectrum. (2) CO₂ was injected into core samples at a constant flow rate of 0.05mL/min with back pressure of 25MPa and 5MPa at 363.15K until no more oil production, then testing T_2 spectrum after CO₂ flooding.

Nuclear magnetic resonance (NMR) had been widely used in the field of core experimental analysis as an efficient, nondestructive and rapid technology to describe fluid quantity and its distribution. According to the relaxation mechanism of NMR, the lateral relaxation time was composed of three parts: surface relaxation time (T_{2s}), bulk relaxation time (T_{2B}), and diffusion relaxation time (T_{2D}). The equation is as follows:

$$\frac{1}{T_2} = \frac{1}{T_{2B}} + \frac{1}{T_{2S}} + \frac{1}{T_{2D}} = \frac{1}{T_{2B}} + \rho_2 \frac{S}{V} + \frac{D(\gamma GT_E)^2}{12} \quad (1)$$

Where ρ_2 was surface relaxation rate, $\mu\text{m} / \text{ms}$, S is Internal surface area of rock pores, μm^2 , V is the pore volume, μm^3 , D was diffusion coefficient of the fluid, $\mu\text{m}^2 / \text{ms}$, γ was Magnetic rotation ratio of hydrogen nuclei, MHz / T, G was magnetic field gradient, G/cm and T_E was Echo interval, ms.

In a uniform magnetic field (corresponding to a small magnetic field gradient), the volume relaxation time (T_{2B}) of the fluid was between 2-3 seconds, which was much greater than the lateral relaxation time T_2 , and the TE value was also small. Therefore, the volume relaxation time (T_{2B}) and diffusion relaxation time (T_{2D}) could be

ignored, and the T_2 relaxation time was mainly determined by surface relaxation (equation 2).

$$\frac{1}{T_2} = \frac{1}{T_{2s}} = \rho_2 \frac{S}{V} = \frac{1}{\rho_2 F_r} r \quad (2)$$

Where F_r was form factor. It could be seen that the transverse relaxation time of fluid in the pore throat space of rock sample was related to the pore throat radius and the form factor of the pore throat body. Therefore, there was a corresponding relationship between the transverse relaxation time of the pore throat and the pore throat radius. Thus, the pore size of core samples could be divide into three sections, small pores ($T_2 < 1\text{ms}$), middle pores ($1\text{ms} \leq T_2 < 10\text{ms}$) and large pores ($T_2 \geq 10\text{ms}$).

2.3 VOF method

VOF method was tracking fluid flow in Euler grids by studying the fluid to mesh volume ratio function within the grid element. For the construction of pore scale grid models, CT scanning was used to reconstruct pore structure, then the grid of the core was obtained by CT grayscale value. Finally, the attribute model of the digital core was obtained through the porosity and permeability parameters. We used the following assumptions to simulate immiscible flooding: (1) There were two types of immiscible and incompressible fluids in the pore network model, (2) The capillary pressure in the network model was inversely proportional to the capillary radius, (3) The fluid satisfies the Poisson's flow equation, (4) Only one fluid interface could exist in the pore grid. The process of CO_2 flow could be described by the Navier-Stokes. CO_2 miscible flooding was described by PR method and fugacity method.

3. RESULTS AND DISCUSSION

3.1 Experimental results and discussion

Fig. 2 showed the oil recovery and gas-oil ratio of CO_2 miscible and immiscible flooding. Oil recovery increase rapidly with the increase of CO_2 injection volume before reaching the inflection point, and the gas-oil ratio before the inflection point was relatively low. CO_2 breakthrough with oil recovery rate of 23.42% after injecting 0.38 PV CO_2 in CO_2 immiscible flooding. Then oil recovery rate increased slowly, with final recovery rate of 34.62% and gas-oil ratio of $2700 \text{ m}^3/\text{m}^3$. For CO_2 miscible flooding, oil recovery reached 57.17% as reaching the inflection point, and the final oil recovery reached 71.28%, more than twice that of CO_2 immiscible flooding.

The T_2 spectrums before CO_2 flooding and after CO_2 flooding were presented in Fig. 3. The T_2 spectrum before

miscible flooding showed a single peak, indicated that oil mainly distributed in middle pores and large pores. After CO_2 miscible flooding, the T_2 spectrum showed double peak characteristics, indicated that residual oil distributed in small pores and large pores. The T_2 spectrum of immiscible flooding exhibited double peaks characteristic before and after CO_2 immiscible flooding, corresponded that oil distribute in small and large pores.

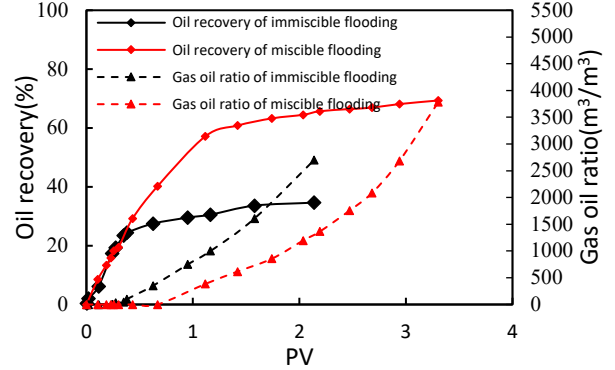


Fig. 2. Oil recovery and gas oil ratio in displacement process with injected CO_2 volume

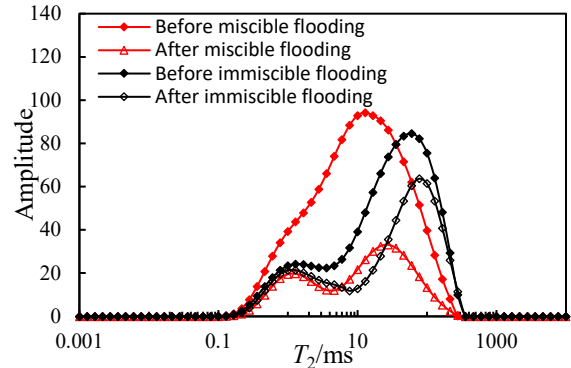


Fig. 3. T_2 spectrum of CO_2 flooding

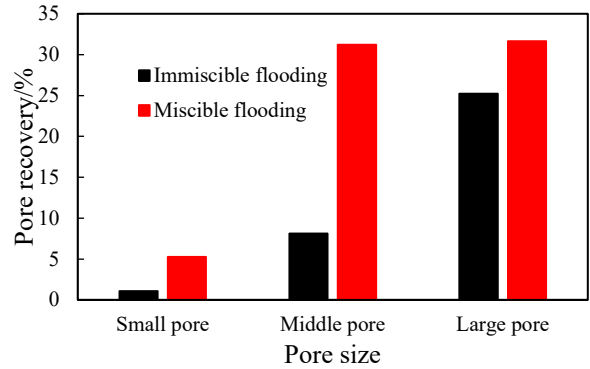


Fig. 4. Oil recovery in different pores

Furthermore, Fig. 4 showed the oil recovery in different kinds of pores. For CO_2 immiscible flooding, oil mainly came from large pores, with oil recovery of 25.2%. In other words, the oil in the small pores had not been displaced. The main displacement mechanism of CO_2 immiscible flooding was the displacement effect of CO_2 and the dissolution of a little of CO_2 in oil to reduce the viscosity. It was difficult for CO_2 to displace oil in small

pores because of the high capillary pressure. For CO₂ miscible flooding, we could observe that the oil recovery in small pores and middle pores is improved significantly. Only the displacement mechanisms of immiscibility and miscibility were considered in this process with same temperature. A large amount of CO₂ dissolved in the oil as pressure was higher than minimum miscibility pressure. The IFT and capillary effect between CO₂ and oil disappeared, and increased the sweep efficiency. Oil recovery of small pores was still relatively low because the diffusion and mass transfer of CO₂ were greatly limited in small pores. Therefore, middle pores and large pores still contributed most of the oil.

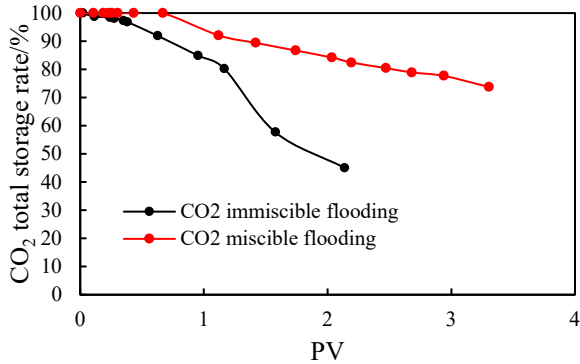


Fig. 5 CO₂ storage of miscible/immiscible flooding

Another interesting result was about CO₂ storage in CO₂ flooding process. As showed in Fig. 5, the CO₂ storage of miscible flooding was much higher than that

of immiscible flooding. Otherwise, it can be observed that after CO₂ breakthrough, the CO₂ storage of immiscible flooding decreased rapidly, and the reducing rate was much faster than that of miscible flooding. There were two main reasons for this phenomenon: the density and solubility of CO₂ increase with the increase of pressure. And the miscibility between CO₂ and oil results in higher diffusion capacity of CO₂, leading to higher dissolution storage of CO₂. On the other hand, oil recovery of CO₂ miscible was higher, allowing for more pores space for CO₂ storage.

3.2 Simulation results and discussion

Fig. 6 distributed the flow characteristics, oil recovery and CO₂ storage of CO₂ miscible and immiscible flooding, from the results of VOF numerical simulation, we observed a significant fingering phenomenon in CO₂ immiscible flooding. And the interesting observation was that piston displacement happened at the injection part and finger displacement became more obvious as closed to the production part during CO₂ miscible flooding. This may be due to the reduction of pressure from the injection to the production, or because of the heterogeneity of the core. Fig. 6c presented the oil recovery in miscible/immiscible flooding, and we could see that the oil recovery of miscible flooding was 52.91%, more than twice that of immiscible flooding which was constant to the experimental results.

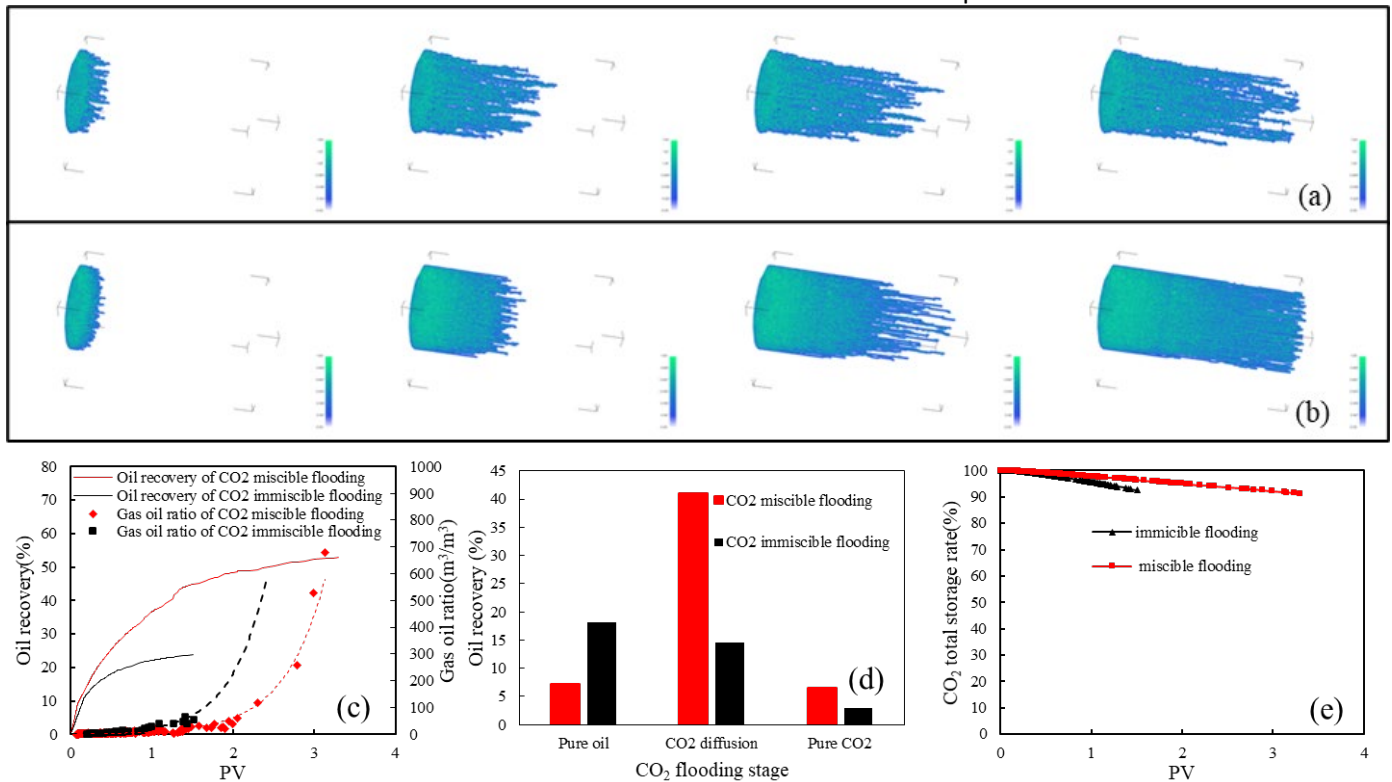


Fig. 6 Characteristic of CO₂ flooding (a. CO₂ flow of immiscible flooding, b. CO₂ flow of miscible flooding, c. Oil recovery and gas oil ratio of CO₂ flooding, d. Oil recovery in different CO₂ flooding area, e. CO₂ storage of CO₂ flooding)

Moreover, the oil recovery curves of CO₂ flooding exhibited three periods, which could be divided into pure oil, diffusion and pure CO₂ area [21]. In CO₂ miscible flooding, during pure oil area, oil recovery curve was an approximate straight line, and there is no gas production. Then oil recovery curve was a logarithmic curve, with a slower growth rate of recovery rate and low gas oil ratio during diffusion area. Finally, in pure CO₂ area, the growth rate of oil recovery further decreased. At the same time, the gas-oil ratio rapidly increased. Oil mainly originated from the diffusion and mass transfer of CO₂ in miscible flooding (Fig. 6d), and pure oil area contribute most oil in immiscible flooding. Fig. 6d showed CO₂ storage in CO₂ miscible/ immiscible flooding, the CO₂ storage of miscible flooding was much higher than that of immiscible flooding with same conditions.

Fig. 7 showed the CO₂ displacement characteristics

under the conditions of oil viscosity of 1 cp, 2 cp and 10 cp, respectively. It could be seen that there was a significant piston displacement in the early period of CO₂ flooding, and as the CO₂ migration distance increases, it gradually showed a fingering phenomenon as oil viscosity of 1 cp. As the increase of oil viscosity, fingering phenomenon appeared earlier and became more significant. At the same time, oil recovery under different oil viscosities also confirmed this phenomenon showed in Fig. 7d. Oil recovery decreased with the increase of oil viscosity. This was due to the increase in oil viscosity, which led to a corresponding increase in oil mobility and a decrease in gas-oil mobility ratio. As a result, the irregular leading edge of gas drive affects CO₂ sweep efficiency, leading to a decrease of oil recovery. Moreover, Fig. 7e showed the CO₂ storage with oil recovery. CO₂ storage increase with the increase of oil recovery.

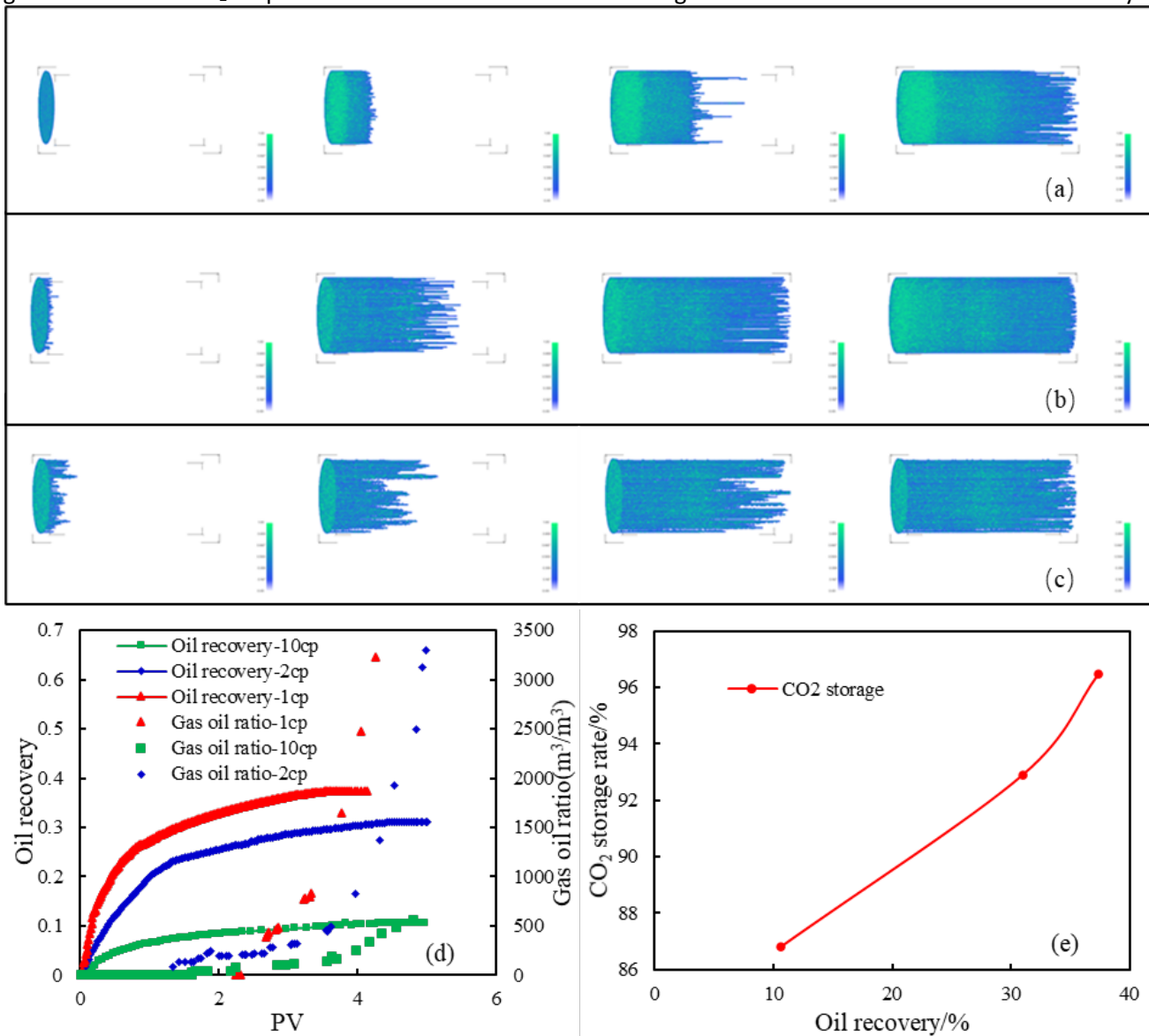


Fig. 7 Characteristic of CO₂ flooding with different viscosity (a. CO₂ flow with oil viscosity of 1cp, b. CO₂ flow with oil viscosity of 2cp, c. with oil viscosity of 10cp, d. Oil recovery and gas oil ratio of CO₂ flooding, e. CO₂ storage of CO₂ flooding)

4. CONCLUSIONS

Laboratory analysis and VOF simulation of CO₂ flooding were conducted, and the main conclusions are as follows:

Oil recovery of CO₂ miscible flooding almost doubled that of CO₂ immiscible flooding. And oil may come from all kinds of pores in miscible flooding. Large pores contributed most oil in CO₂ immiscible flooding. CO₂ storage in immiscible flooding was lower than that in miscible flooding, and decreased more rapidly after CO₂ break through than that in miscible flooding.

VOF simulation results showed that finger displacement appears in CO₂ immiscible flooding, and piston displacement happened at the injection part and finger displacement did at the production part during CO₂ miscible flooding.

Oil recovery of CO₂ miscible flooding is twice as much as the one of immiscible flooding which are dependent on the characteristic of CO₂-oil contact. Oil recovery and storage of CO₂ flooding significantly decreased with the increase of oil viscosity.

ACKNOWLEDGEMENT

This research was conducted with financial support from the Youth Science and Technology Innovation Team of Southwest Petroleum University (No. 2018CXTD10) and the National Natural Science Foundation Project of China (No. 51874248 and No. U19B2010). We would like to show our deepest appreciation to them all for their support and help.

DECLARATION OF INTEREST STATEMENT

The authors declare that they have no known competing financial interests or personal relationships that could have appeared to influence the work reported in this paper. All authors read and approved the final manuscript.

REFERENCE

[1] Bashir A, Haddad AS, Rafati R. A review of fluid displacement mechanisms in surfactant-based chemical enhanced oil recovery processes: Analyses of key influencing factors. *Pet Sci* 2021; 19(3): 1211-1235. <https://doi.org/10.1016/j.petsci.2021.11.021>

[2] Jia C, Zou C, Yang Z, Zhu R, Chen Z, Zhang B, et al. Significant progress of Continental Petroleum geological theory in basins of Central and Western China. *Pet Explor Dev* 2018; 45(4): 573-588. [https://doi.org/10.1016/S1876-3804\(18\)30064-8](https://doi.org/10.1016/S1876-3804(18)30064-8)

[3] Machale J, Majumder SK, Ghosh P, et al. Development of a novel biosurfactant for enhanced oil recovery and its

influence on the rheological properties of polymer. *Fuel* 2019; 257: 116067. <https://doi.org/10.1016/j.fuel.2019.116067>

[4] Li HT, Li Y, Chen SN, et al. Effects of chemical additives on dynamic capillary pressure during waterflooding in low permeability reservoirs. *Energy Fuels* 2016; 30 (9), 7082-7093. [10.1021/acs.energyfuels.6b01272](https://doi.org/10.1021/acs.energyfuels.6b01272)

[5] Kang WL, Zhou BB, Issakhov M, et al. Advances in enhanced oil recovery technologies for low permeability reservoirs. *Petro Sci* 2022; 19:1622-1640. <https://doi.org/10.1016/j.petsci.2022.06.010>

[6] Zhao FL, Zhang L, Hou JR, et al. Profile improvement during CO₂ flooding in ultra-low permeability reservoirs. *Petrol Sci*, 2014; 11(2):279-286. <https://doi.org/10.1007/s12182-014-0341-6>

[7] Li S, Qiao C, Li Z, Hui Y. The effect of permeability on supercritical CO₂ diffusion coefficient and determination of diffusive tortuosity of porous media under reservoir conditions. *J CO₂ Utiliz* 2018; 28:1-14. <https://doi.org/10.1016/j.jcou.2018.09.007>

[8] Othman F, Naufaliansyah MA, Hussain F. Effect of water salinity on permeability alteration during CO₂ sequestration. *Adv Water Resour* 2019; 127:237-51. <https://doi.org/10.1016/j.advwatres.2019.03.018>

[9] Kamari A, Arabloo M, Shokrollahi A, et al. Rapid method to estimate the minimum miscibility pressure (MMP) in live reservoir oil systems during CO₂ flooding. *Fuel* 2015; 153, 310-319. <https://doi.org/10.1016/j.fuel.2015.02.087>

[10] Torabi F, Qazvini FA, Kavousi A, Asghari K. Comparative evaluation of immiscible, near miscible and miscible CO₂ huff-n-puff to enhance oil recovery from a single matrix-fracture system (experimental and simulation studies). *Fuel* 2012; 93: 443-53. <https://doi.org/10.1016/j.fuel.2011.08.037>

[11] Zhou X, Yuan Q, Zhang Y, Wang H, Zeng F, Zhang L. Performance evaluation of CO₂ flooding process in tight oil reservoir via experimental and numerical simulation studies. *Fuel* 2019; 236:730-46. <https://doi.org/10.1016/j.fuel.2018.09.035>

[12] Wang TF, Wang LL, Meng XB, et al. Key parameters and dominant EOR mechanism of CO₂ miscible flooding applied in low-permeability oil reservoirs. *Geo Sci Eng*. 2023; 225: 211724. <https://doi.org/10.1016/j.geoen.2023.211724>.

[13] Wei B, Zhang X, Wu RN, et al. Pore-scale monitoring of CO₂ and N₂ flooding processes in a tight formation under reservoir conditions using nuclear magnetic resonance (NMR): A case study. *Fuel*, 2019; 246: 34-41. <https://doi.org/10.1016/j.fuel.2019.02.103>.

[14] Cai MY, Su YL, Hao YM, et al. Monitoring oil

- displacement and CO₂ trapping in low-permeability media using NMR: A comparison of miscible and immiscible flooding. *Fuel* 2021; 305: 121606. <https://doi.org/10.1016/j.fuel.2021.121606>
- [15] Tora G., Hansen A., Oren P. Dynamic network modeling of resistivity index in a steady-state procedure. SPE135367-MS, 2010. <https://doi.org/10.2118/135367-MS>
- [16] Sochi T. Pore-scale modeling of non-newtonian flow in porous media. *Physics* 2007; 51(22): 5007-5023. <https://doi.org/10.48550/arXiv.1011.0760>
- [17] Chen H., Chen S., Mathaeus W.H. Recovery of the Navier-Stokes equation using a lattice gas Boltzmann method. *Physical Review A* 1992; 45(8): 5339-5342. <https://doi.org/10.2307/3185570>
- [18] Liu H., Valocchi A. J., Werth C., et al. Pore-scale simulation of liquid CO₂, displacement of water using a two-phase lattice Boltzmann model. *Advances in Water Resources* 2014; 73: 144-158.
- [19] Blunt M. J., Bijeljic B., Dong H., et al. Pore-scale imaging and modelling. *Advances in Water Resources*, 2013, 51(1): 197-216. <https://doi.org/10.1016/j.advwatres.2012.03.003>
- [20] Sun HX, Yao J, Zhao YJ. Water displacement characteristics at high water-cut stage based on microscopic experiments and simulations. *Simulation* 2019; 97(2): 155-166. 10.1177/0037549719831361.
- [21] Wang HL, Tian L, Huo MH, et al. Dynamic track model of miscible CO₂ geological utilizations with complex microscopic pore-throat structures. *Fuel* 2022; 322: 124192. <https://doi.org/10.1016/j.fuel.2022.124192>